Master Sintering Curve for a Two-Phase Material

D.C. Blaine, S. Park and R.M. German

Center for Innovative Sintered Products, The Pennsylvania State University, University Park, PA, USA

Abstract

A new two-phase master sintering curve model for sintering densification of gas-atomized 17-4PH stainless steel, with consideration of δ-ferrite content, is developed. A phase transition from α-austenite to δ-ferrite starts at 1200°C in 17-4PH stainless steel, changing the rate of densification significantly during sintering from this point on. The conventional master sintering curve concept has difficulty describing this phenomena accurately. The new two-phase master sintering curve is characterized by two temperature regions with two corresponding activation energies and two different rates of densification. This new concept can be easily extended to other sintering systems with two or multiple phases. The newly developed sinter model is shown to predict density evolution for a MIM compact during sintering in an industrial pusher furnace. The predicted final density shows good agreement with experimentally measured values.

1. Introduction

The master sintering curve (MSC) is a simple and effective sinter model, used to predict the sintering densification of a porous body formed from powder. Sinter models, using the MSC approach, have been determined for powder ceramics as well as for powder metals [1,2]. These studies have shown that the MSC is a powerful tool in helping determine the dominant sintering mechanisms through diffusional activation energy analysis, as well as providing a predictive model for estimating density as a function of thermal cycle (time and temperature profile). However, most of these experiments have been conducted on materials that do not change phase during sintering and under laboratory conditions. There can be significant differences in sintering results when scaling up to manufacturing conditions. In this study, the MSC for injection molded, gas-atomized 17-4PH stainless steel, determined from laboratory dilatometry experiments, is used to predict sinter density for samples of varying size in an industrial pusher furnace. In this way, the model is tested in an industrial setting and shown to be accurate. The implication of these results is that a MSC developed under laboratory conditions can be used with confidence to design and control sinter cycles for industrial conditions. Two forms of the MSC were explored in this study: firstly, the conventional form of the MSC, where one activation energy is prescribed to the entire thermal cycle; and secondly, a two-phase form of the MSC that takes into account the enhanced sintering experienced around 1200°C with the appearance of a δ-ferrite, high diffusivity phase in 17-4PH stainless steel. Previous research on 17-4PH stainless steel [3] identified the effect of δ-ferrite on the sintering kinetics, linking the sintering activity to the microstructure.

2. Experimental

2.1. MSC characterization experiments

The MSC is characterized by a series of constant heating rate or isothermal hold sintering experiments [1]. In this study, constant heating rate experiments were conducted in a vertical pushrod dilatometer (Anter Corporation). The samples for the experiments were cut from the gates of injection molded bars. The injection molding feedstock was compounded using gas-atomized 17-4PH stainless steel, for which the powder characteristics are given in Table 1, at 55vol.% solids loading with the Powderflo® water-based agar binder system.

particle size	D_{10}	D_{50}	D_{90}
laser diffraction, wet measurement	4.74μm	10.21μm	16.95μm
density	apparent	tap	pycnometer
	3.75g/cm^3	4.63g/cm^3	7.69g/cm^3

Table 1. Powder characteristics for gas-atomized 17-4PH stainless steel

The samples were debound in retort furnaces (Lindberg) under flowing hydrogen using the following thermal cycle: 2°C/min ramp to holds at 60°C, 1h; 110°C, 1h; and 600°C, 2h consecutively, followed by cooling in the furnace at 5°C/min to room temperature. Six dilatometer tests, run in hydrogen, were conducted in total: three (cycles 1, 4, 5) to characterize the lower temperature (<1200°C) behaviour and three (cycles 1, 2, 3) for the higher temperature behaviour. The thermal profiles for the tests are reported in Table 2. The sintering shrinkage measured in the dilatometer for each of these cycles is shown in Figure 1.

cycle	**ramp 1**	**hold 1 (1h)**	**ramp 2**	**hold 2 (1h)**
1	10°C/min	1010°C	7°C/min	1365°C
2	10°C/min	1010°C	5°C/min	1365°C
3	10°C/min	1010°C	1.67°C/min	1365°C
4	7°C/min	1200°C	-	-
5	5°C/min	1200°C	-	-

Table 2. Dilatometer sinter cycles for characterization experiments

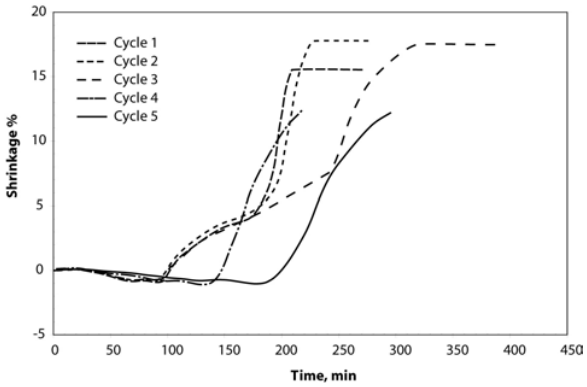

Figure 1. Dilatometer shrinkage results for MSC characterization experiments, with thermal cycles given in Table 2.

2.2. MSC verification experiments

Sintering experiments were conducted in an industrial pusher furnace (CM Furnaces) to verify the MSC model for gas-atomized 17-4PH stainless steel. Samples of varying size were cut from injection molded rectangular bars for this purpose, giving five samples at each of the five sizes shown in Table 3. The dimensions of the samples have been rounded to the nearest 0.5mm and the standard deviation on measurements was less than 0.2mm. The samples were dried at 60°C for 1h in a convection oven, in air.

sample ID	dimensions, mm	density, g/cm^3
LB	170.5 x 17.5 x 10	4.81 ± 0.02
A	36 x 17.5 x 13.5	4.78 ± 0.05
B	12.5 x 12 x 12	4.73 ± 0.02
C	31 x 17.5 x 10	4.72 ± 0.02
D	18 x 10 x 10.5	4.73 ± 0.04

Table 3. Verification experiment sample data (green)

The pusher furnace used to run the verification experiments has six preheat zones and three high heat zones of 670mm each. The preheat and high heat zones are separated by a 335mm transitional zone. The furnace was run at a push rate of 7.5mm/min under flowing hydrogen, with the temperature set points for the zones given in Table 4.

cycle → zone ↓	A	B	C	D	E
preheat 1	90				
preheat 2	180				
preheat 3	350				
preheat 4	500				
preheat 5	650				
preheat 6	950				
high heat 1	1000	1000	1000	1000	1150
high heat 2	1100	1100	1200	1200	1300
high heat 3	1100	1200	1200	1300	1320

Table 4. Zone temperatures (°C) for pusher furnace

After sintering, the samples were measured and weighed. The sinter density was evaluated using the Archimedes water immersion method for groups A – D, group LB was too large to use this method so the dimensions and mass were used for this calculation. The sinter density and final shrinkage results are presented in Figure 2. The reported data is an average of the different size samples from Table 3, with one sample of each size used per thermal cycle given in Table 4. The final shrinkage reported for each experiment is the average over all five size samples of the average measured shrinkage in the length, width and height.

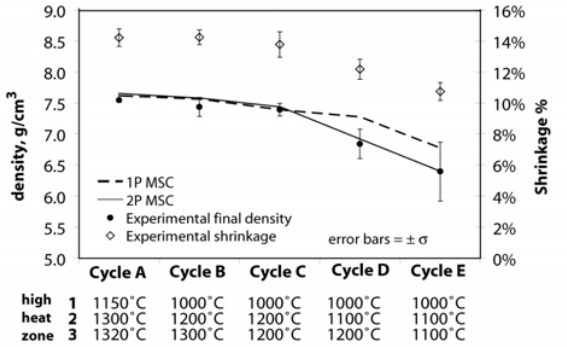

Figure 2. Shrinkage and final density results of pusher furnace verification experiments, showing comparison of MSC model predicted final density.

3. Model

3.1. Conventional MSC

The conventional MSC as defined by Johnson [1], links the time-temperature (*t-T*) integral, sometimes called the work-of-sintering θ [4],

$$\theta = \int_0^t \frac{1}{T}\exp\left(-\frac{Q}{RT}\right)dt \qquad (1)$$

to the relative sinter density, ρ at time t during the thermal cycle, starting at $t = 0$. In this study, the relative sinter density will be reported with respect to the theoretical density of the powder, given in Table 1 as 7.69g/cm^3. The units of time and temperature used for calculation are seconds and Kelvin, respectively. The activation energy Q for the sintering system is either determined through minimizing the error between the experimental data and the model, or it is assigned a value based on known diffusional activation energy for the system [1,4]. It has been shown [2,4] the a sigmoid function provides a good fit between the relative sinter density and the natural logarithm of the work-of-sintering, ln θ. The sigmoid equation used to define the MSC is

$$\rho = \rho_o + \frac{1-\rho_o}{1+\exp\left(-\frac{\ln\theta + a}{b}\right)} \qquad (2)$$

where ρ_o is the relative density at the start of the sintering experiment, and a and b are constants defining the curve. For this study, the activation energy was determined to be $Q = 350kJ/mol$, with constants $a = 29.93$ and $b = 1.521$.

3.2. Two-phase MSC

To incorporate the effects of the enhanced sintering experienced in this system, the model was split into two

regions: a low temperature (<1200°C) and high temperature (>1200°C) region. For this material system, the two regions are defined, based on Equation 2, by the following two equations:

low temperature region (<1200°C):

$$\rho_1 = 0.55 + \frac{0.45}{1+\exp\left(-\frac{\ln\theta_1 + 26.48}{2.006}\right)} \quad (3)$$

where θ_1 is calculated as in Equation 1 with Q_1 = *321kJ/mol*.

high temperature region (>1200°C):

$$\rho_2 = 0.55 + \frac{0.45}{1+\exp\left(-\frac{\ln\theta_2 + \chi}{0.09512}\right)} \quad (4)$$

where the work-of-sintering θ_2 is calculated from 1200°C with Q_2 = *350kJ/mol*, i.e.

$$\theta_2 = \theta_1\left(1200^\circ C, t_{1200^\circ C}\right) + \int_{1200^\circ C}^{t} \frac{1}{T}\exp\left(-\frac{Q_2}{RT}\right)dt \quad (5)$$

The χ parameter in the high temperature region defined by Equation 4 is not a unique point in θ as it is dependent on the thermal history (ramp and holds) of the low temperature region. It is determined by setting the low and high temperature equations equal to each other at 1200°C. For instance, for a 2°C/min ramp from 30°C to 1200°C, $\theta_1 = 4{\cdot}10^{-10}$*s/K* and setting Equation 3 and 4 equal to each other at this point gives a value for χ = *28.45*. Figure 3 shows the MSC plot for this hypothetical case.

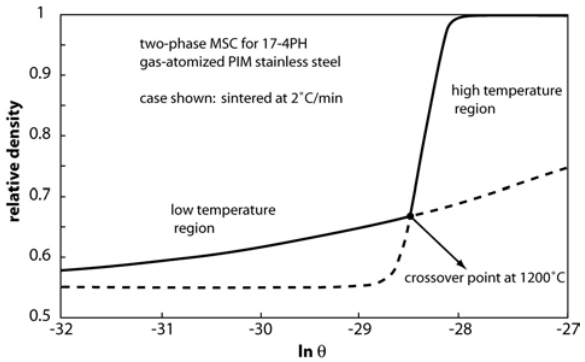

Figure 3. Two-phase MSC showing crossover from low temperature region to high temperature region, characterized by Equations 3 and 4, respectively.

4. Results

To evaluate the accuracy of the MSC, the experimentally measured sinter density was compared with the predicted density, determined from the models given in Equations 3 and 4. In all cases, both the original single phase (1P MSC) and two-phase (2P MSC) models predicted the density within one standard deviation range about the mean value, seen in Figure 1.

The two-phase MSC gave a marginally better error at 2.82%, compared to the single phase MSC with an error of 0.89%. However, it should be noted that this error was calculated by comparing the final density predictions to the measured values only, and not as a sum of the errors over the entire sintering regime.

When comparing experimental dilatometry results with the predictive model, it is clear that the two-phase MSC gives a closer prediction across the entire thermal cycle, as shown in Figure 4.

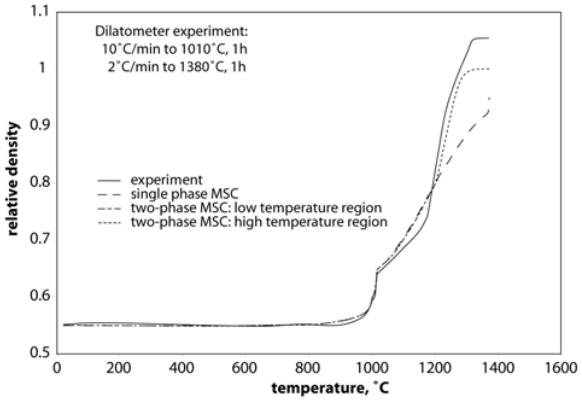

Figure 4. Comparison of dilatometry experiment and predicted density using both original and two-phase MSC.

The data in Figure 4 corresponds to a dilatometer experiment using a sample prepared in the same way described in this paper, and sintered at 10°C/min to 1010°C with a 1h hold, followed by a 2°C/min ramp to 1380°C with a 1h hold at this temperature. The sum of the squared errors gives 3.938 for the single phase MSC, while the two-phase MSC gives 0.680 for this dilatometer experiment. The final density measured by Archimedes water immersion test was 100%, however, the final shrinkage measured (compensating for thermal expansion with *CTE = 14.8ppm/°C*) was 20.5%. Assuming isotropic shrinkage and applying conservation of mass calculations, this corresponds to a final density of 109%. Obviously, this is not possible. It is assumed that the force of the dilatometer pushrod is causing a small degree of anisotropic shrinkage, thus measured shrinkage includes some creep deformation as well as sintering shrinkage. This explains the misleading experimental data in Figure 4.

5. Conclusions

17-4PH gas-atomized stainless steel, injection molded using an agar binder, has been used as a demonstration material for the evaluation of the MSC sinter model. Both the original MSC sinter model, as well as a newly developed form of the MSC that allows for incorporation of a two-phase sintering response have been presented here. The models were characterized using laboratory scale dilatometry experiments, and then tested through verification experiments run on an industrial pusher furnace. It was found that the both the original MSC and the two-phase MSC both provide good prediction of the final density, however the two-phase MSC provides a more accurate prediction of the sinter density point by point over the thermal cycle.

References:

[1] Su, H. and Johnson, D.L., Master Sintering Curve: A Practical Approach to Sintering, *J. Am. Ceram. Soc.*, 1996, **79**, (12), 3211-3217

[2] Teng, M-H., Lai, Y-C. and Chen, Y-T., A Computer Program of Master Sintering Curve Model to Accurately Predict Sintering Results, *West. Pac. Earth Sc.*, **2**, (2), 171-180

[3] Wu, Y., Blaine, D., Marx, B., Schlaefer, C. and German, R.M., Sintering Densification and Microstructure Evolution of Injection Molding Grade 17-4PH Stainless Steel Powder, *Met. Mat. Trans. A.,* 2002, **33A**, 2185-2194

[4] Blaine, D.C., Gurosik, J.D., Park, S-J., Heaney, D., and German, R.M., Master Sintering Curve Concepts as Applied to the Sintering of Molybdenm, *Met. Mat. Trans. A.,* 2005, in press